

# Link Fraction Mixed Membership Reveals Community Diversity in Aggregated Social Networks

Gamal Adel<sup>1</sup>, Eszter Bokányi<sup>1</sup>, Eelke M. Heemskerk<sup>2</sup>, Frank W. Takes<sup>1</sup>

February 4, 2026

## Abstract

Community detection is a critical tool for understanding the mesoscopic structure of large-scale networks. However, when applied to aggregated or coarse-grained social networks, disjoint community partitions cannot capture the diverse composition of community memberships within aggregated nodes. While existing mixed membership methods alleviate this issue, they may detect communities that are highly sensitive to the aggregation resolution, not reliably reflecting the underlying community structure of the underlying individual-level network. This paper presents the Link Fraction Mixed Membership (LFMM) method, which computes the mixed memberships of nodes in aggregated networks. Unlike existing mixed membership methods, LFMM is consistent under aggregation. Specifically, we show that it conserves community membership sums at different scales. The method is utilized to study a population-scale social network of the Netherlands, aggregated at different resolutions. Experiments reveal variation in community membership across different geographical regions and evolution over the last decade. In particular, we show how our method identifies large urban hubs that act as the melting pots of diverse, spatially remote communities.

## 1 Introduction

One of the most characteristic properties of large-scale social networks is their community structure, as it can reveal social tendencies and association patterns within a population at the mesoscale level (Backstrom et al., 2006). Communities, groups of individuals that are more connected to each other than with other groups, can provide insight into social network mechanisms such as homophily (Menyhért et al., 2024), segregation (Kazmina et al., 2024), and information spread (Mantzaris, 2014). However, evaluating the community structure of individual-level social networks is often untenable, as such data may be inaccessible due to privacy concerns or being too computationally expensive to process. (Peng et al., 2018; Jong et al., 2024).

As a common alternative, aggregated (coarse-grained) networks are typically constructed by partitioning nodes into disjoint sets (e.g., through clustering or grouping by geographical and affiliation attributes) and then summing up edge counts or weights between nodes in these sets (Kim, 2004). While aggregation destroys much of the individual-level information of the network, it has been shown that it can give large-scale insights about the underlying network (Butts, 2009). However, there is currently a lack of tools specifically designed for properly analyzing aggregated networks, resulting in many existing works in the literature simply treating them as weighted networks (Gandica et al., 2018). The main problem with applying weighted network analysis methods to aggregated data assumes, explicitly or otherwise, that each aggregated set is an indivisible unit and that findings on the set apply to its constituent nodes. Such an assumption is termed an ecological fallacy, where findings on groups of individuals are extended to the individuals themselves (Robinson, 2009).

The above-mentioned handling of aggregated networks is especially problematic for community detection methods. Few works applying community detection on aggregated datasets have attempted to confirm whether the community structure is conserved upon disaggregation. Instead, the relevance of these findings to the underlying individuals is either ignored or simply taken for granted (Butts, 2009; Gandica et al., 2018). Applying a disjoint community detection algorithm, where each aggregated set gets classified under one community, is problematic for at least three reasons. First, even in individual-level social networks, a categorical membership for a single community can be an oversimplification of an overlapping state of membership of several communities (Yang et al., 2014; Kuppevelt et al., 2020). The extent and composition of this overlap can be a distinguishing feature of nodes, reflecting the roles different nodes have in connecting the communities. (Evans et al., 2009). Second, this oversimplification is exacerbated further in aggregated networks. When an entire group of individuals in an aggregated set is subject to one community classification, information is lost about the composition of its constituents' membership in other communities. Gandica et al., showed that detected disjoint community partitions over aggregated networks can be significantly sensitive to the partition and resolution of the aggregation, resulting in community classifications that are unstable across different aggregations (Gandica et al., 2018). Sensitivity to the scale and shape of aggregation is a well-documented challenge, known as the Modifiable Areal Unit Problem (MAUP) (Wong, 2004). Third and finally, it can be challenging to observe changes in community membership of nodes, as the disjoint classification of membership occludes small but meaningful changes (Xing et al., 2008; Peixoto, 2015). In aggregated networks, lacking the ability to distinguish these changes in membership hinders efforts to understand changes of membership composition of aggregated nodes and also the evolution of the community structure as a whole (Rosvall et al., 2010; Cazabet et al., 2023).

Different methods have been proposed to address some of these concerns. Mixed membership methods allow nodes to belong to multiple communities simultaneously, reflecting their

latent-space position or their probability of belonging to a set of communities (Xing et al., 2008; E. M. Airoldi et al., 2015; Poux-Médard et al., 2023). Various approaches exist in the literature, such as the Mixed Membership Stochastic Block-Model (MMSBM) (E. Airoldi et al., 2007) and overlapping SBM (Peixoto, 2019), which use causal inference to estimate these membership values. Some have adapted this approach to aggregated relational data (Jones et al., 2021; Ward et al., 2025). However, these methods still fail to address the ecological fallacy of categorizing an aggregated set, and in turn, all nodes within that set, under the same label, leaving them vulnerable to instability under aggregation. MMSBM, for example, assumes that the node is an indivisible unit in some latent space of community memberships, not an aggregation of nodes from an underlying network.

To address this issue, we propose the Link Fraction Mixed Membership (LFMM) for community detection in aggregated networks. The method defines the membership of a node in a given community as the total link volume connecting to nodes within that community. Unlike other mixed membership methods, LFMM results in membership values that are conserved across any possible aggregation or disaggregation. More specifically, we prove that LFMM results on an aggregated network equal the sum of LFMM values computed on the disaggregated network. LFMM also stands out for being computable in a single matrix multiplication, being applicable to directed and weighted networks, and being compatible with any community detection algorithm. The method’s sensitivity to aggregation is examined through numerical experiments on synthetic benchmark networks.

Then we utilize LFMM to investigate the community structure and evolution in a real-world aggregated population-scale social network of the Netherlands. The dataset is a register-based social network of all 17 million residents and the different types of affiliations (family, work, and school) connecting them, over 13 years (Bokányi et al., 2023; van der Laan, 2022). Only the aggregated forms of the network, where residents are grouped based on their residential addresses within approximately 3000 neighbourhoods and 400 municipalities, are examined. While previous studies have identified disjoint, space-independent communities in a static Dutch social network of the Netherlands (Menyhért et al., 2024), this work uses a mixed membership approach to investigate community diversity and yearly evolution over a decade. When applying LFMM, we find that mixed membership is heterogeneously distributed but strongly influenced by geospatial patterns. When accounting for the spatial factor using a gravity null model, we find that highly urban regions act as melting pots where members of different communities reside. Finally, we uncover significant longitudinal changes in the community structure and diversity of different regions.

The remainder of this paper is organized as follows. Section 2 formalizes the Link Fraction Mixed Membership (LFMM) method, proves its consistency over aggregation, and defines the metrics used to quantify community diversity and statistical significance. In Section 3, we present the population-scale social network of the Netherlands and apply LFMM to this

dataset, revealing a strong correlation between urbanness and community diversity and capturing the evolution of the community structure. Finally, Section 4 discusses the implications of the method and findings, and outlines directions for future research.

## 2 Methodology and Validation

In this section, we present the Link Fraction Mixed Membership (LFMM) method used to uncover community diversity in aggregated networks. The analytical workflow employed in this study consists of two stages:

1. **LFMM Computation:** LFMM requires applying an arbitrary community detection method to obtain a disjoint partition. It then evaluates mixed membership vectors for each aggregated node by computing the fraction of links connecting that node to each community (Section 2.1).
2. **Diversity and Significance Analysis:** We quantify the heterogeneity of these membership vectors using a community diversity index and evaluate their statistical significance against a null model (Section 2.2).

The code for the LFMM method and the subsequent analysis can be found on <https://github.com/g-adel/LFMM-Paper>.

### 2.1 Link Fraction Mixed Membership

The conceptual foundation of LFMM rests on a link-centric perspective of network structure, where a node’s identity is defined by the distribution of its interactions. By defining mixed membership as the fraction of link volume connecting a node to a community, LFMM captures the association of a node or aggregate set with a community. Consequently, the method can be interpreted as a single-step diffusion process, representing the probability that a random walker starting at a node or set of nodes will land within a specific community. This approach draws upon the intuition that the node’s role in networks is determined by its connectivity with the various communities, as also proposed in link clustering methods (Ahn et al., 2009; Cho et al., 2014).

The LFMM method requires an initial disjoint partition of the aggregated network. For this study, we employ the Leiden algorithm (Traag et al., 2019) to optimize the Reichardt and Bornholdt’s Potts model (Reichardt et al., 2006). This algorithm is chosen for its theoretical robustness under aggregation (Gandica et al., 2018).

### 2.1.1 LFMM formulation

We assume there is a hidden disaggregated weighted and undirected network  $G = (V, E, W)$  which can be presented as an adjacency matrix  $w$  where  $w_{uv}$  is the weight of the edge between nodes  $u$  and  $v$ . Instead of  $G$ , we are given a graph  $G'$ , obtained from the aggregation of a partition of the nodes of  $G$  into  $n$  disjoint *aggregation sets*  $S_1, \dots, S_n$ .  $G'$  has  $n$  nodes, and its edge weights  $w'_{ij}$  are defined as the sum of edges/weights in  $G$  between nodes in the corresponding aggregation sets  $S_i$  and  $S_j$ :

$$w'_{ij} = \sum_{u \in S_i, v \in S_j} w_{uv}. \quad (1)$$

For self-loops,  $w'_{ii}$  is the number of half-edges within set  $S_i$ .

Finally, we introduce the mixed membership vector  $M$ . For a node  $i$  in the original graph, the unnormalized membership  $M_i$  of community  $k$  and its normalized form  $m_i$  are defined as:

$$M_i(k) := \sum_{j \in C_k} w_{ij} \left(1 - \frac{\delta_{ij}}{2}\right), \quad m_i(k) := \frac{M_i(k)}{\sum_k M_i(k)}, \quad (2)$$

Here  $\delta$  is the Kronecker delta. The normalized mixed-membership formulation  $m_i(k)$  can be described as the link-weight fraction of node  $i$  towards all other nodes labeled under community  $k$ , including internal connections, as illustrated in Figure 1a.

Analogously, for an aggregate set  $S_x$ , we define the aggregate mixed membership  $M'_x$  and its normalized form  $m'_x$  using the aggregated weights:

$$M'_x(k) := \sum_{j \in C'_k} w'_{xj} \left(1 - \frac{\delta_{xj}}{2}\right), \quad m'_x(j) := |S_x| \frac{M'_x(k)}{\sum_k M'_x(k)} \quad (3)$$

The unnormalized mixed membership matrix for the entire network can be calculated via a single matrix multiplication of the aggregated adjacency matrix and a community indicator matrix. Furthermore, an extension of the method as a diffusion process that accounts for higher order connectivity can be computed through exponentiating the matrix. The formal matrix multiplication operation and its exponentiation is provided in Appendix A.

### 2.1.2 LFMM consistency under aggregation

A key property of LFMM is that, due to the linearity of the formulation, it is consistent under aggregation. More specifically, it can be proven that for an aggregated set  $S_x$ , the sum of the mixed membership vectors  $M_i$  of its constituent nodes results in the same values as computation of the mixed membership on the aggregated set  $M_x$ :

$$\begin{aligned}
\sum_{i \in S_x} M_i(k) &= \sum_{i \in S_x} \left( \sum_{j \in C_k} w_{ij} \left( 1 - \frac{\delta_{ij}}{2} \right) \right) \\
&= \sum_{Y \in C'_k} \left( \sum_{i \in S_x} \sum_{j \in S_Y} w_{ij} \left( 1 - \frac{\delta_{ij}}{2} \right) \right) \\
&= \sum_{Y \in C'_k} w'_{xY} \left( 1 - \frac{\delta_{xY}}{2} \right) = M'_x(k)
\end{aligned} \tag{4}$$

This consistency is illustrated in Figure 1b, which contrasts two potential computational pathways to arrive at the mixed membership values in the aggregate network. Starting from a disjoint community partition of the aggregated network, the first path (red arrow) represents the direct application of LFMM. The second path (black arrows) represents a theoretical process where the community partition is disaggregated to the individual-level network, LFMM is computed for every node, and then aggregated back. Because the definition of  $M$  behaves linearly, these two pathways are mathematically equivalent. Consequently, computing membership on the aggregate is guaranteed to yield the exact same total mass as if we had access to the micro-level graph and summed the memberships of all constituent nodes. This property ensures that the method is robust against the specific scale of aggregation, a trait not shared by non-linear mixed membership definitions.

A major caveat for this definition is that it is edge-centric, meaning that nodes with higher node degree/strength will play a larger role in the mixed membership of its aggregated set. For this case, the normalized forms  $m_i$  and  $m'_x$  were introduced. However,  $m$  and  $m'$  do not share the same relationship as  $M$  and  $M'$ . Instead,  $m'_x$  can be formulated as a weighted sum of nodes proportional to their strengths.

### 2.1.3 Synthetic Networks and Benchmarks

To validate and analyze the consistency of the LFMM method and its robustness against aggregation, we generated synthetic networks using the Stochastic Block Model (SBM) (Abbe, 2018). We construct a graph  $G$  with  $N = 1,000$  nodes divided into  $r = 2$  communities. The affinity parameter  $\mu$  dictates the proportional probability of forming connections to outside the community, with an average degree of 20. To simulate the aggregation process, nodes are uniformly classified under one of  $n = 50$  aggregate sets  $\mathbf{S}$  with a mixing probability  $m$  of being assigned to a random aggregate set instead.

We perform three comparisons to evaluate the consistency of LFMM after applying community detection using the Leiden Algorithm (Traag et al., 2019), visualizing the correlation between values computed directly on the aggregated network  $G'$  and those derived from the

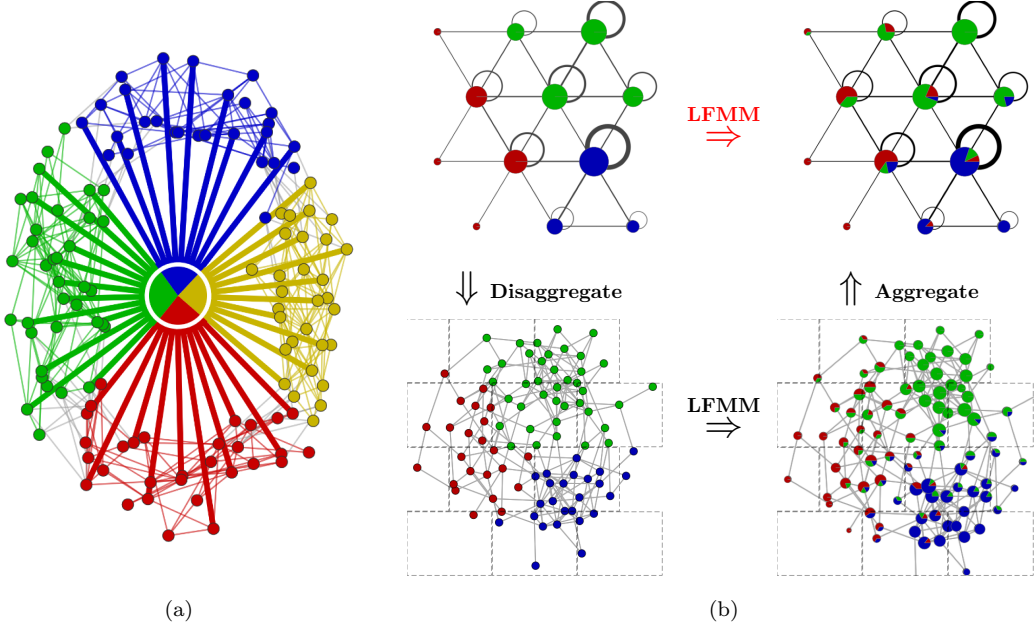


Figure 1: *Link Fraction Mixed Membership (LFMM) method and its consistency under aggregation.* (a) Computing the link fraction of a node as fraction of connections to nodes within different community partitions. (b) Starting from an aggregated network with colored detected communities (top left): LFMM can be applied directly (red path) and be guaranteed to be equivalently computed by disaggregating communities to the individual level, computing LFMM, and aggregating back (black path). The dotted rectangles denote the aggregation partitioning of the individual-level network.

individual-level network  $G$ . First, we validate the conservation property (eq. 4) by comparing the raw LFMM vector  $M'$  (as defined in Section 2.1) computed on  $G'$  against the sum of individual vectors  $M$  computed on  $G$  (using the community partition from the aggregate network). Second, we repeat this comparison for the sum of normalized vectors  $m$  versus  $m'$  to assess deviations caused by the normalization of mixed membership vector. Finally, we compare the aggregate LFMM results against a "ground truth" scenario where community detection is performed on the individual-level graph  $G$  rather than  $G'$ .

The results are displayed in Figure 2a. The raw LFMM values (blue) exhibit a perfect correlation ( $r = 1.0$ ), empirically confirming that the method is mathematically consistent under aggregation. The normalized values (orange) show a high but imperfect correlation ( $r \approx 0.999$ ), as the normalization by node strength does not scale linearly with aggregation. The comparison with the individual-level detection (green) demonstrates that LFMM applied to aggregated data ( $r \approx 0.997$ ) also serves as a reasonable approximation of the underlying micro-scale community structure, though shows a bias of over-estimating the minority membership in aggregated nodes. Practically, this bias occurs when attempting to capture the unknown

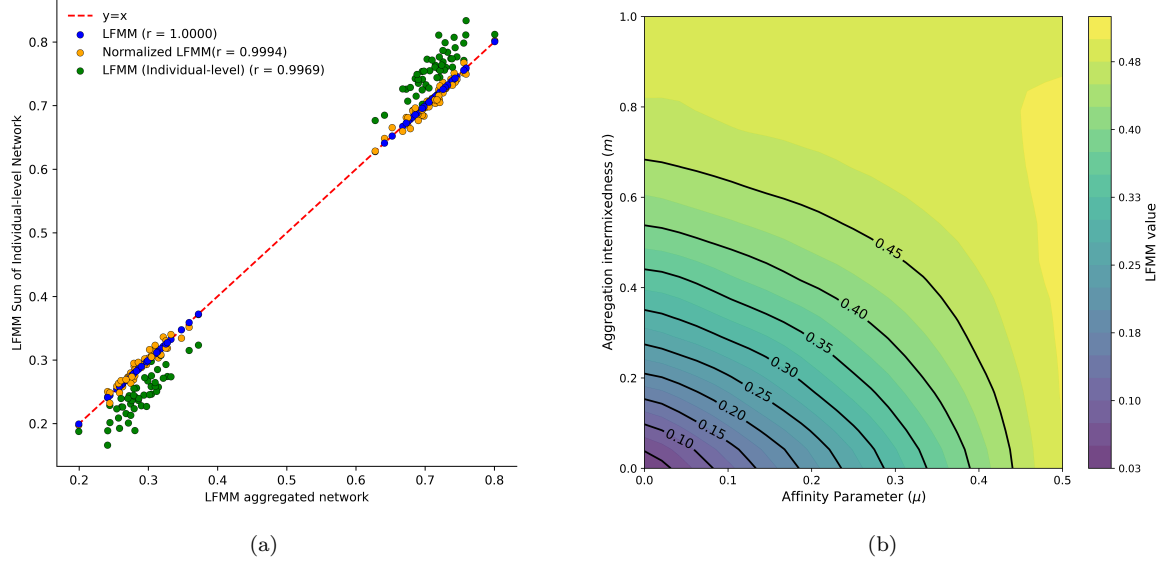


Figure 2: *LFMM consistency under aggregation and community affinity.* (a) Sum of mixed memberships computed on the synthetic individual-level network ( $m = 0.2$ ) versus the mixed memberships computed directly on the aggregated network. **Blue:** LFMM values ( $M$ ) following disaggregation then reaggregation. **Orange:** Normalized LFMM values ( $m$ ). **Green:** LFMM of community detection performed at the individual level. (b) Isoline contour plot of mean LFMM value for different values of affinity ( $\mu$ ) and aggregation intermixedness  $m$ .

community structure at the individual-level, as suboptimal partitioning creates a deviation between the aggregated and individual scales.

When evaluating the mean values of LFMM for synthetic networks of various affinity parameters and aggregation mixing, we find that mixed membership highly correlates with either affinity or mixing when the other factor is absent (see Figure 2b). However, when combined, there is a nearly symmetric effect of both factors on the mixed membership values. This happens because high aggregation mixing (aggregated sets that contain a heterogeneous mix of members of both communities) results in a similar link fraction akin to a well-aggregated network (homogeneous sets) that has high affinity. In other words, under the assumption of a disjoint community structure in the individual layer, LFMM does not distinguish between an aggregated set that is heterophilically connected and one that is heterogeneously mixed. Consequently, distinguishing which is the source of high mixed membership can only be made through inspecting the method of aggregation and the uniformity of community membership within the aggregated set.

## 2.2 Community diversity and statistical significance

For the purposes of empirically testing LFMM on a large-scale social network in Section 3, we describe two necessary metrics for evaluating membership diversity and statistical significance.

First, to measure the overall diversity of community memberships within a given aggregate set, we employ the Gini-Simpson Index (GSI) (Jost, 2006). Given the normalized mixed membership vector  $\vec{m}_i$  for an aggregate set  $i$ , the GSI is calculated as:

$$GSI(\vec{m}_i) = 1 - \sum_{j=1}^r m_i(j)^2. \quad (5)$$

Here  $r$  is the total number of communities. In the context of an aggregate set, GSI represents the probability that two individuals, drawn at random from the aggregate set  $S$ , belong to different communities. The index ranges from 0 (single community) to a theoretical maximum of  $1 - 1/r$  (uniform distribution). A high GSI value thus corresponds to a high degree of local co-existence between members of different communities. While this diversity metric is directly proportional to the total minority membership fraction, it distinguishes two high minority fractions based on how heterogeneous the membership distribution is.

Second, to isolate the component of diversity that is not explained by geographic proximity, we compute the statistical significance of the GSI diversity, via the  $z$ -score, as compared to a gravity null model (Prieto Curiel et al., 2018). This metric compares the empirically observed GSI with the expected GSI mean and variance derived from the gravity null model. The  $z$ -score  $z_i$  for aggregate set  $i$  is defined as:

$$z_i = \frac{GSI_i - \mu_i}{\sigma}. \quad (6)$$

Here,  $\mu$  and  $\sigma$  are the gravity null model mean and standard deviation for the set. A  $z$ -score value near zero indicates that the observed diversity value is expected based on the region's relative geographic location and population.

### 3 Community mixed membership in the Dutch social network

In this section, we present the aggregated social network of the Netherlands and empirical results obtained by applying the proposed Link Fraction Mixed Membership method. We provide two sets of analyses. The first pertains to the computation and analysis of mixed membership values, in comparison with disjoint community partitions, and tracking community evolution over time. The second evaluates the diversity of community memberships, distinguishing between spatially-driven and socially-driven heterogeneity. In the latter, we utilize a spatial null model to identify significant diversity patterns and link them to the level of urbanization in different regions.

### 3.1 Population-scale Social Network of the Netherlands

We utilize the register-based population-scale social network of the Netherlands. This dataset is constructed from yearly administrative registers covering the entire population of the country (approximately 17 million residents and 1 billion edges each year). The network captures formal social ties defined by government records, including family relationships (first- and second-degree relatives, partners), school affiliations (primary, secondary, vocational school, and university year groups), household connections, next-door neighbors, and work relationships (colleagues) (van der Laan, 2022; Bokányi et al., 2023). By combining these layers, the network represents the "social opportunity structure" of the population (Soler et al., 2024; Bokányi et al., 2023).

For the purposes of this study, we focus on two spatial aggregations of the above individual-level networks, based on people's residential addresses within *neighborhoods*, which are in turn part of *municipalities*. This results in two undirected weighted networks per year: a neighborhood-aggregated network and a municipality-aggregated network, where edge weights represent the sum of all types of social ties between residents of any two regions. Since household and next-door neighbor connections almost never cross neighborhood boundaries by definition, we omit them from our analysis. For family, school, and work connections, our aggregation preserves the internal connectivity within each administrative unit (i.e., number of half-edges between residents of the same neighborhood) as self-loops. Access to this value is necessary for the conservation property of the LFMM method.

The network is available for each year from 2009 to 2021, allowing for the analysis of the evolution of community structure over time. For analysis results of a single year, we focus on the 2021 snapshot of the network (1.6 billion edges over 3218 neighborhoods or 352 municipalities). Administrative boundaries defining these aggregation sets are not static; municipal re-divisions, mergers, and border adjustments occur often, which consequently alters the composition of the aggregation sets across snapshots.

### 3.2 Mixed membership in the Dutch social network

We first identify the large-scale community structure using a disjoint community detection on the municipality-aggregated network of the population-scale social network of the Netherlands. The resulting partition (Figure 3a) and the community-aggregated adjacency matrix (Figure 3b) reveal a strong spatial embedding, with communities forming geographically contiguous territories that closely align with provincial administrative borders, similar to other findings in the literature (Robiglio et al., 2025; Menyhért et al., 2024; Kallus et al., 2015). Communities were named after the province or administrative region with which they had most nodes in common (e.g., the green community is labeled "Utrecht-aligned community" as it is centered around the province).

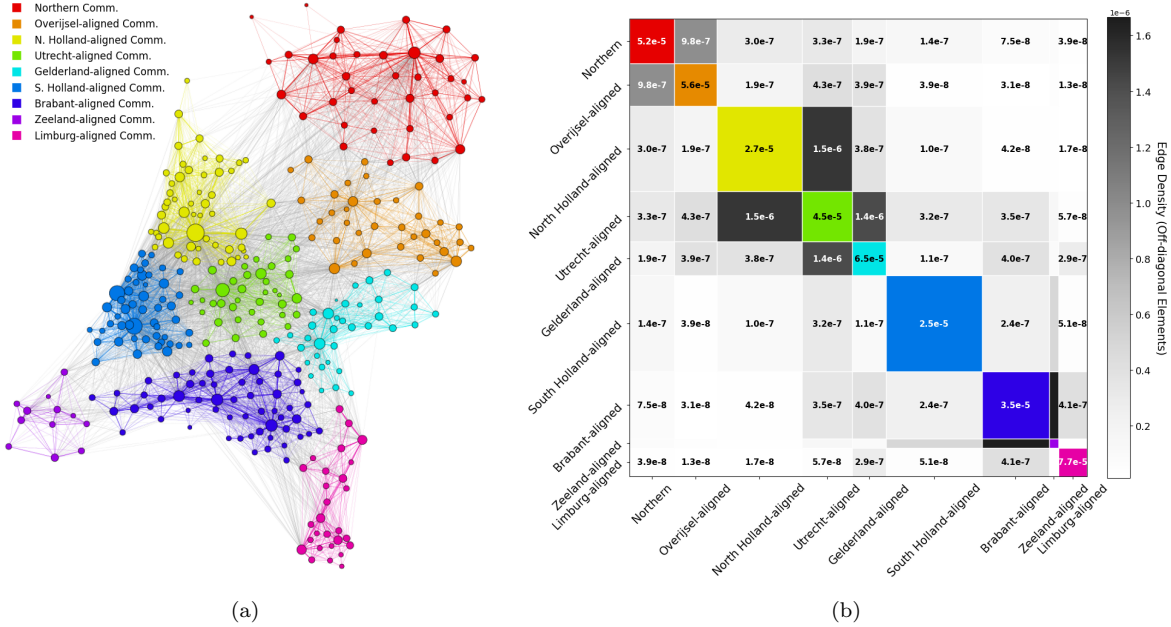


Figure 3: *Disjoint community structure of the population-scale network of the Netherlands* **(a)** Community partition of the municipality-aggregated network. Node sizes are proportional to population, colors represent community membership. Communities are named after the provinces they most closely match. **(b)** Community-aggregated adjacency matrix showing the density of connections within (diagonal) and between (off-diagonal) communities. Block sizes are proportional to community population. The matrix is ordered to minimize off-diagonal density values.

To investigate the internal composition of these regions, we applied LFMM (as defined in Section 2.1) to obtain the mixed-membership composition for each municipality (Figure 4). The resulting membership distribution improves upon the limitations of the disjoint partition described above. While the disjoint algorithm enforces a sharp boundary between communities, the LFMM results show that municipalities situated on opposite sides of these detected borders exhibit similar mixed membership profiles. The mixed membership view also shows that spatial proximity drives a continuous transition of community influence, rather than discrete territories. However, certain deviations from spatial patterns can be observed, namely in a distinction between rural and urban areas. While rural municipalities are largely dominated by a single community membership, major urban centers such as Utrecht, Amsterdam, and Rotterdam display a noticeably more heterogeneous composition of non-local memberships, as can be seen in Figure 4a. However, to rule out the possibility that this pattern is merely an artifact of the municipalities' size and geographic centrality, we validate this observation against a spatial null model in Section 3.3. The mixed membership values for the 40 largest municipalities can be found in the Appendix 1.

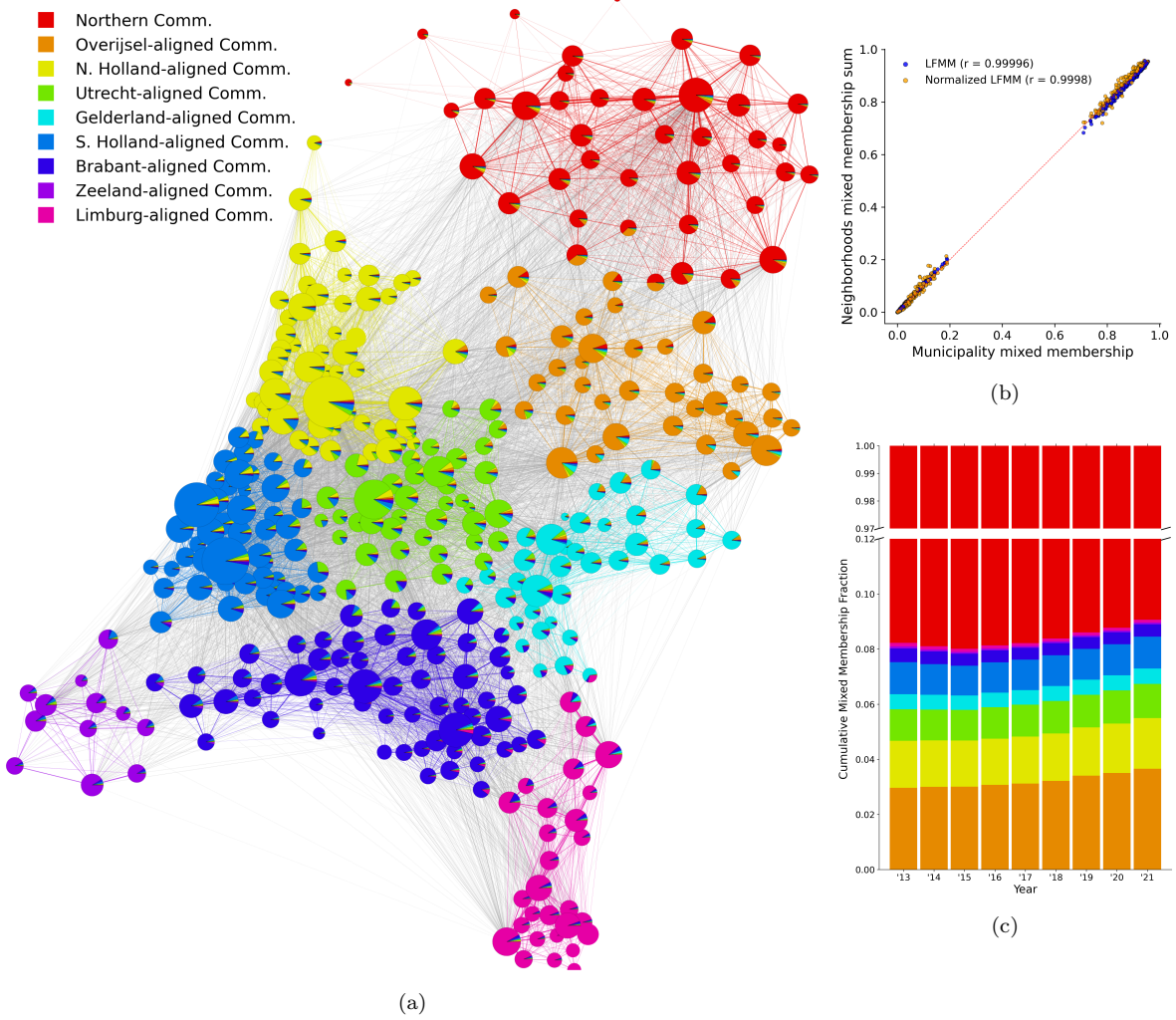


Figure 4: *Mixed membership community composition and analysis.* (a) The Dutch municipality-aggregated network. Each node is represented by a pie chart showing the distribution of its mixed membership vector, sized proportional to population. Colors correspond to the communities identified in Figure 3. (b) Comparison of LFMM values computed directly on the municipality-aggregated network (vertical axis) versus the sum of LFMM values computed on the neighborhood network (horizontal axis). (c) Temporal evolution over a decade of the total mixed membership mass within the northern (red) community, broken down by target community affiliation.

After having investigated the method’s consistency across different scales of aggregation on simulated data in Section 2.1.3, we now do so empirically on the Dutch network in Figure 4b. We observe that the mixed membership values computed directly on the coarser municipality network are nearly identical to the sum of the values computed on the finer neighborhood network (Pearson correlation  $\rho > 0.999$ ). This confirms that LFMM is robust against the aggregation level of the network, preserving the total “mass” of community

membership regardless of whether the network is analyzed at the neighborhood or municipal scale.

Finally, the method enables the analysis of gradual community evolution that are unobservable in the disjoint partitioning. Figure 4c tracks the evolution of total mixed membership within the northern community over a decade. We observe gradual changes in the community composition, such as the rising influence of the neighboring Overijssel-aligned (orange) community and the decline of connections to the southern provinces. This demonstrates the method’s capacity to capture slow shifts in the mesoscale network structure over time not visible through traditional methods.

### 3.3 Community diversity

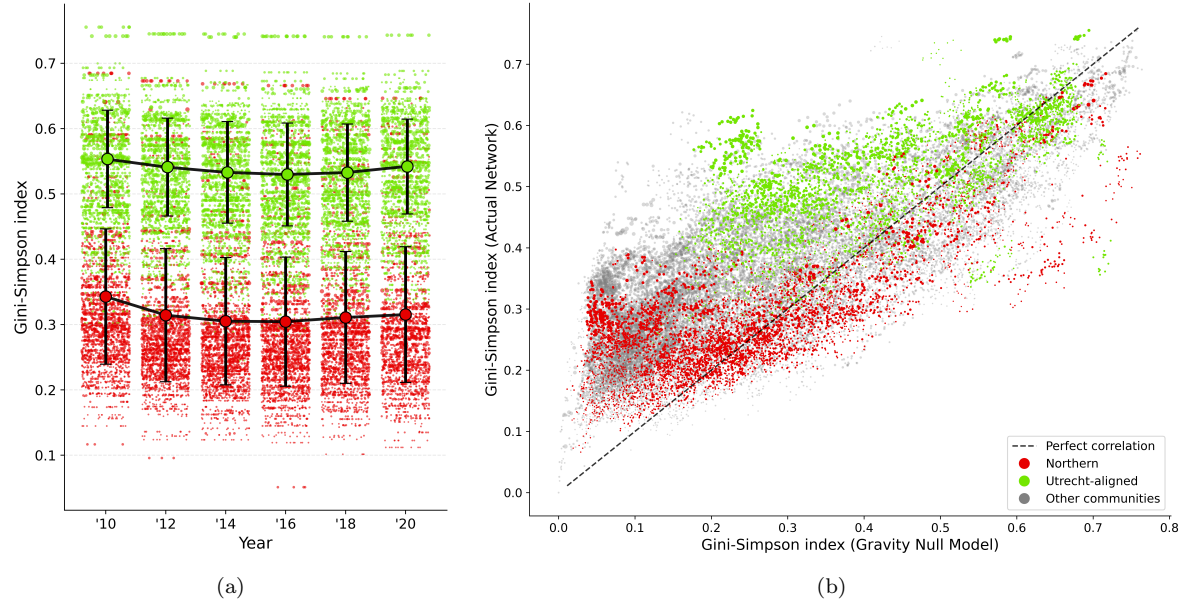


Figure 5: *Community diversity in the neighborhood-aggregated network over time.* (a) Temporal evolution of the Gini-Simpson diversity index (GSI) diversity of neighborhoods in the Utrecht-aligned (green) and Northern (red) communities from 2010 to 2020. Points are neighborhoods and scaled by population size. (b) GSI for each neighborhood in the observed network (vertical axis) versus the GSI expected from the gravity null model (horizontal axis). Points near the dashed diagonal line have a diversity value that is expected by the null model.

We quantify the heterogeneity of community composition within each municipality through employing the GSI diversity index (as defined in Section 2.2) on the mixed membership values. First, in Figure 5a, we inspect the evolution of diversity of neighborhoods in the Utrecht-aligned and northern communities over a decade. Significant changes in mean diversity were observed in both communities, with a significant drop from 2010 values that is partially re-

covered later on by the Utrecht-aligned community. Second, since we are interested in how the diversity of neighborhoods within different communities compare both to one another and to a spatial null model, we plot the observed diversity against the diversity expected from the gravity null model in Figure 5b. A strong correlation is evident, confirming that the relative geographic location is a primary determinant of a region’s diversity. For instance, centrally located communities like the Utrecht-aligned community exhibit high diversity in the null model and somewhat higher values in the observed network, simply due to their proximity to multiple other communities. Conversely, peripheral communities like the northern community show low expected diversity. However, many neighborhoods exhibit diversity scores significantly higher than what the gravity model predicts, suggesting the presence of social forces beyond spatial considerations. This deviation is not uniform across communities; for example, while neighborhoods in the northern community cluster at low expected diversity values, a subset of them diverges from the diagonal, indicating much higher actual diversity than their geography would predict.

To identify the neighborhoods with sufficiently high diversity that is unaccounted for through spatial factors, we compute the statistical significance of the diversity through the  $z$ -score (see Section 2.2). Visualizing the  $z$ -score on a map (Figure 6a) effectively removes the sensitivity to community borders and reveals a clear pattern: significant diversity is concentrated in and around the nation’s largest cities. Amsterdam, The Hague, and Rotterdam emerge as prominent hot spots. Notably, Groningen also stands out, exhibiting exceptionally high diversity given its geographically remote location. This may reflect that, being a traditional student city, Groningen attracts young people from across the country.

This relationship is further quantified in Figure 6b, which shows a strong positive correlation between a neighborhood’s  $z$ -score and its population density. This effect is further amplified by the urbanization level of the surrounding municipality. This finding indicates that urban environments act as melting pots, facilitating a level of community mixing that significantly exceeds the baseline interaction predicted by physical proximity. Notably, this metric highlights the unique position of Groningen. Despite its geographic isolation (resulting in low absolute diversity), it exhibits the highest  $z$ -score in the country ( $z = 2.36$ ,  $GSI=0.30$ ), identifying it as a highly integrative hub relative to its spatial constraints. It is followed closely by the major cities of the Randstad conurbation, including The Hague ( $z = 2.35$ ), Delft ( $z = 2.15$ ), and Amsterdam ( $z = 1.98$ ). The fact that the method identifies these known urban centers as statistically significant outliers confirms LFMM’s capacity to detect complex social connectivity patterns in aggregated data.

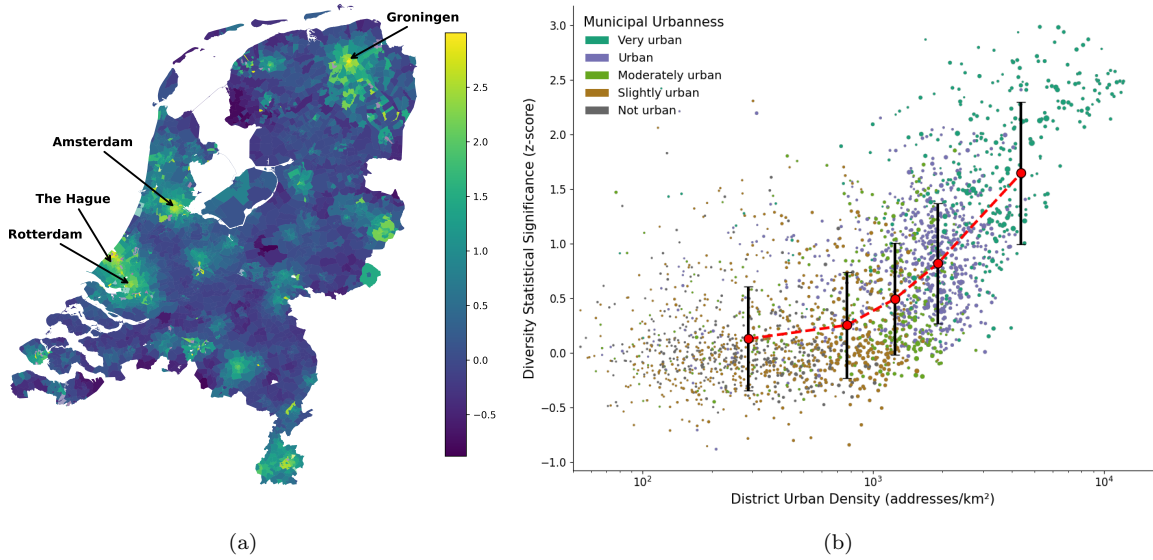


Figure 6: *Community diversity statistical significance and its link to urbanization.* (a) Geographic heatmap of the  $z$ -score of community diversity across neighborhoods. Hot spots of high diversity (yellow) are clearly concentrated in major urban areas. (b) Neighborhood diversity statistical significance vs urban density, colored by their parent municipality urbanization level. A strong positive trend indicates that denser, more urban regions are significantly more diverse than what a spatial model alone predicts.

## 4 Discussion and Conclusion

Our analysis of the population-scale social network of the Netherlands demonstrates that traditional disjoint community detection, while capturing spatial administrative boundaries, fails to represent intermixed aggregated social networks. This confirms that treating aggregated sets as indivisible units risks obscuring the underlying network structure. The proposed Link Fraction Mixed Membership (LFMM) method resolves this by treating an aggregate node as a sum of diversely-connected nodes rather than an atomic unit. By ensuring that membership sums are conserved under aggregation and disaggregation, LFMM provides a consistent link between the macroscale aggregated network and the microscale heterogeneity of the individual-level graph. This consistency allows for a robust analysis that is not strictly bound by the specific resolution or shape of the aggregation partition.

We validated the utility of the method by applying it to the population-scale social network of the Netherlands. While the raw mixed membership values largely reflected the strong spatial embedding of the network, the integration of a gravity null model allowed us to disentangle diversity arising from geographic proximity from that driven by social preference.

Applying the method to the population-scale social network of the Netherlands revealed that, while raw mixed membership values largely reflected the network’s strong spatial em-

bedding, the integration of a gravity null model allowed us to disentangle diversity arising from geographic proximity from that driven by social preference. This distinction was crucial for identifying that high levels of significant diversity are notably correlated with urbanization. The finding that urban centers function as "melting pots" demonstrates that LFMM is capable of detecting subtle, non-spatial structural patterns that are typically dominated by the geographic constraints of the network.

Some caution is necessary, however, when interpreting these mixed membership results. The edge-centric nature of the method offers a distinct perspective. Because the membership vectors are weighted by node strength, they reflect the volume of connectivity within a region rather than the number of residing individuals. While this means that high-degree hubs may disproportionately influence the aggregate profile, it provides a meaningful measure of connectivity between groups. Furthermore, while the properties of LFMM as a mixed membership method holds true for any aggregated network, it does not distinguish between an aggregated set that is heterophilically connected and a heterogeneously mixed aggregated set. Consequently, the accuracy of this estimation requires further evaluation across real and synthetic networks with varying topologies.

Future work could focus on benchmarking LFMM against inference-based approaches, such as Mixed Membership Stochastic Block Models (MMSBM), to explore which conceptual definitions of membership are most suitable for different analytical goals. Additionally, the versatility of the method should be tested on a broader range of network types, including directed, weighted, multiplex, and link-partitioned networks. Ultimately, LFMM enables the robust analysis of community composition and dynamics, especially in (spatially) aggregated temporal networks. By uncovering community composition diversity and evolution, it facilitates our understanding of the complex structure and dynamics of communities in large-scale networks.

## References

Abbe, E. (2018). “Community detection and stochastic block models: recent developments”. In: *Journal of Machine Learning Research* 18.177, pp. 1–86.

Ahn, Y.-Y., J. P. Bagrow, and S. Lehmann (2009). “Link communities reveal multiscale complexity in networks”. In: *Nature* 466, pp. 761–764. DOI: 10.1038/nature09182.

Airoldi, E. et al. (2007). “Mixed Membership Stochastic Blockmodels”. In: *Journal of Machine Learning Research* 9, pp. 1981–2014. DOI: 10.1145/1134271.1134283.

Airoldi, E. M. et al. (2015). *Handbook of mixed membership models and their applications*. CRC press Boca Raton, FL. DOI: 10.1145/1134271.1134283.

Backstrom, L. et al. (2006). “Group formation in large social networks: membership, growth, and evolution”. In: *Proceedings of the 12th ACM SIGKDD international conference on Knowledge discovery and data mining*. New York, NY, USA: Association for Computing Machinery, pp. 44–54. DOI: 10.1145/1150402.1150412.

Bokányi, E., E. M. Heemskerk, and F. W. Takes (2023). “The anatomy of a population-scale social network”. In: *Scientific Reports* 13.1, p. 9209. DOI: 10.1038/s41598-023-36324-9.

Butts, C. T. (2009). “Revisiting the foundations of network analysis”. In: *Science* 325.5939, pp. 414–416. DOI: 10.1126/science.1171022.

Cazabet, R. and G. Rossetti (2023). “Challenges in community discovery on temporal networks”. In: *Temporal network theory*. Springer, pp. 185–202. DOI: 10.1007/978-3-030-23495-9\_10.

Cho, Y.-S., G. Ver Steeg, and A. Galstyan (2014). *Mixed Membership Blockmodels for Dynamic Networks with Feedback*. DOI: 10.1609/aaai.v25i1.7952.

Evans, T. and R. Lambiotte (2009). “Line graphs, link partitions, and overlapping communities.” In: *Physical review E, Statistical, nonlinear, and soft matter physics* 80 1 Pt 2, p. 016105. DOI: 10.1103/physreve.80.016105.

Gandica, Y. et al. (2018). “Measuring the effect of node aggregation on community detection”. In: *EPJ Data Science* 9. DOI: 10.1140/epjds/s13688-020-00223-0.

Jones, T. et al. (2021). “Scalable Community Detection in Massive Networks using Aggregated Relational Data”. In: *arXiv preprint 2108.01727*. DOI: 10.5705/ss.202022.0411.

Jong, R. G. de, M. P. van der Loo, and F. W. Takes (2024). “The effect of distant connections on node anonymity in complex networks”. In: *Scientific Reports* 14.1, p. 1156. DOI: 10.1038/s41598-023-50617-z.

Jost, L. (2006). “Entropy and diversity”. In: *Oikos* 113.2, pp. 363–375. DOI: <https://doi.org/10.1111/j.2006.0030-1299.14714.x>.

Kallus, Z. et al. (2015). “Spatial fingerprints of community structure in human interaction network for an extensive set of large-scale regions”. In: *PLOS ONE* 10.5, e0126713. DOI: 10.1371/journal.pone.0126713.

Kazmina, Y. et al. (2024). "Socio-economic segregation in a population-scale social network". In: *Social Networks* 78, pp. 279–291. DOI: 10.1016/j.socnet.2024.02.005.

Kim, B. J. (2004). "Geographical coarse graining of complex networks." In: *Physical Review Letters* 93 16, p. 168701. DOI: 10.1103/physrevlett.93.168701.

Kuppevelt, D. V. et al. (2020). "Community membership consistency applied to corporate board interlock networks". In: *Journal of Computational Social Science* 5, pp. 841–860. DOI: 10.1007/s42001-021-00145-5.

Mantzaris, A. V. (2014). "Uncovering nodes that spread information between communities in social networks". In: *EPJ Data Science* 3.1, p. 26. DOI: 10.1140/epjds/s13688-014-0026-9.

Menyhért, M. et al. (2024). "Connectivity and community structure of online and register-based social networks". In: *EPJ Data Science* 14, p. 8. DOI: 10.1140/epjds/s13688-025-00522-4.

Peixoto, T. P. (2015). "Inferring the mesoscale structure of layered, edge-valued, and time-varying networks". In: *Physical Review E* 92.4, p. 042807. DOI: 10.1103/physreve.92.042807.

Peixoto, T. P. (2019). "Bayesian stochastic blockmodeling". In: *Advances in network clustering and blockmodeling*, pp. 289–332. DOI: 10.1002/9781119483298.ch11.

Peng, S., S. Yu, and P. Mueller (2018). *Social networking big data: Opportunities, solutions, and challenges*.

Poux-Médard, G., J. Velcin, and S. Loudcher (2023). *Dynamic Mixed Membership Stochastic Block Model for Weighted Labeled Networks*. New York, NY, USA: Association for Computing Machinery, pp. 1569–1577. DOI: 10.1145/3539618.3591675.

Prieto Curiel, R. et al. (2018). "Gravity and scaling laws of city to city migration". In: *PLoS ONE* 13.7, e0199892. DOI: 10.1371/journal.pone.0199892.

Reichardt, J. and S. Bornholdt (2006). "Statistical mechanics of community detection". In: *Physical Review E* 74.1, p. 016110. DOI: 10.1103/physreve.74.016110.

Robiglio, T. et al. (2025). "Multiscale patterns of migration flows in Austria: regionalization, administrative barriers, and urban-rural divides". In: *arXiv preprint 2507.11503*. DOI: 10.48550/arXiv.2507.11503.

Robinson, W. S. (2009). "Ecological correlations and the behavior of individuals". In: *International Journal of Epidemiology* 38.2, pp. 337–341. DOI: 10.1093/ije/dyn357.

Rosvall, M. and C. T. Bergstrom (2010). "Mapping change in large networks". In: *PLoS ONE* 5.1, e8694. DOI: 10.1371/journal.pone.0008694.

Soler, N., E. Heemskerk, and Y. Kazmina (2024). "Contacts in contexts: Measuring intergroup contact opportunities at the population-scale through linked administrative and survey data". In: DOI: 10.31235/osf.io/axumt.

Traag, V. A., L. Waltman, and N. J. Van Eck (2019). “From Louvain to Leiden: guaranteeing well-connected communities”. In: *Scientific Reports* 9.1, pp. 1–12. DOI: 10.1038/s41598-019-41695-z.

van der Laan, J. (2022). *A Person Network of the Netherlands*. [https://www.cbs.nl/-/media/\\_pdf/2022/20/person\\_network\\_netherlands.pdf](https://www.cbs.nl/-/media/_pdf/2022/20/person_network_netherlands.pdf).

Ward, O. G., A. L. Smith, and T. Zheng (2025). “Bayesian Modeling for Aggregated Relational Data: A Unified Perspective”. In: *arXiv preprint 2506.21353*. DOI: 10.5705/ss.202022.0411.

Wong, D. W. (2004). “The modifiable areal unit problem (MAUP)”. In: *WorldMinds: geographical perspectives on 100 problems: commemorating the 100th anniversary of the association of American geographers 1904–2004*. Springer, pp. 571–575. DOI: 10.4135/9780857020130.n7.

Xing, E., W. Fu, and L. Song (2008). “A state-space mixed membership blockmodel for dynamic network tomography”. In: *The Annals of Applied Statistics* 4, pp. 535–566. DOI: 10.1214/09-aoas311.

Yang, J. and J. Leskovec (2014). “Overlapping communities explain core–periphery organization of networks”. In: *Proceedings of the IEEE* 102.12, pp. 1892–1902. DOI: 10.1109/jproc.2014.2364018.

## A Computation and Extension of LFMM

### A.1 Single matrix computation of LFMM

The mixed membership vectors for all aggregated sets can be computed simultaneously using linear algebra. Let  $n$  be the number of aggregated sets and  $r$  be the number of communities. We define the community indicator matrix  $\mathbf{C}$  of dimension  $n \times r$  as:

$$C_{ij} = \begin{cases} 1 & \text{if } S_i \in C_j \\ 0 & \text{otherwise} \end{cases} \quad (7)$$

Let  $\mathbf{A}'$  be the modified aggregated adjacency matrix of dimension  $n \times n$ . To ensure consistency with the definition of  $M'_x(k)$  in Equation (3), where self-loops contribute with a factor of  $1/2$ , the diagonal elements of  $\mathbf{A}'$  must be scaled. Given that  $w'_{ii}$  represents the number of half-edges within set  $S_i$ , we define:

$$A'_{ij} = \begin{cases} w'_{ij} & \text{if } i \neq j \\ \frac{1}{2}w'_{ii} & \text{if } i = j \end{cases} \quad (8)$$

The unnormalized mixed membership matrix  $\mathbf{M}'$ , where the element  $M'_{ij}$  corresponds to the link weight from set  $i$  to community  $j$ , is then obtained by the matrix multiplication:

$$\mathbf{M}' = \mathbf{A}'\mathbf{C} \quad (9)$$

### A.2 Extension to higher-order diffusion

The formulation above captures direct connectivity, equivalent to a single step of a random walker. To extend LFMM to account for higher-order connectivity over  $t$  discrete steps, we first, we define the diagonal degree matrix  $\mathbf{D}$  where  $D_{ii} = \sum_j A'_{ij}$ . We then construct the row-stochastic transition matrix  $\mathbf{P}$ :

$$\mathbf{P} = \mathbf{D}^{-1}\mathbf{A}' \quad (10)$$

Here,  $P_{ij}$  represents the probability that a random walker at node  $i$  moves to node  $j$  in one step. The normalized mixed membership matrix after  $t$  steps, denoted as  $\mathbf{m}^{(t)}$ , is computed by raising the transition matrix to the power of  $t$  and projecting onto the communities:

$$\mathbf{m}^{(t)} = \mathbf{P}^t\mathbf{C} \quad (11)$$

In this formulation, the element  $m_{ik}^{(t)}$  represents the probability that a random walker starting at aggregated set  $i$  will be located within community  $k$  after exactly  $t$  steps. The standard normalized LFMM corresponds to the case where  $t = 1$ .

## B Municipalities mixed membership

Table 1: Mixed membership of top 40 municipalities by population (2021)

Municipality	Population	Northern	Overijssel	N. Holland	Utrecht	Gelderland	S. Holland	Brabant	Zeeland	Limburg
Amsterdam	870 084	0.007	0.008	<b>0.897</b>	0.029	0.007	0.037	0.011	0.001	0.003
Rotterdam	651 188	0.004	0.005	0.024	0.018	0.005	<b>0.916</b>	0.021	0.004	0.003
's-Gravenhage	548 108	0.005	0.005	0.036	0.016	0.005	<b>0.916</b>	0.012	0.002	0.003
Utrecht	359 118	0.010	0.015	0.063	<b>0.818</b>	0.015	0.045	0.025	0.004	0.006
Eindhoven	235 645	0.003	0.004	0.012	0.015	0.014	0.017	<b>0.897</b>	0.002	0.034
Groningen	233 127	<b>0.912</b>	0.031	0.019	0.013	0.006	0.012	0.005	0.001	0.001
Tilburg	221 952	0.002	0.004	0.010	0.016	0.011	0.023	<b>0.914</b>	0.004	0.017
Almere	214 642	0.014	0.026	<b>0.876</b>	0.041	0.007	0.025	0.008	0.001	0.002
Breda	184 045	0.004	0.005	0.017	0.021	0.010	0.054	<b>0.871</b>	0.008	0.010
Nijmegen	177 371	0.006	0.017	0.015	0.033	<b>0.846</b>	0.014	0.049	0.002	0.018
Apeldoorn	164 731	0.015	<b>0.803</b>	0.025	0.050	0.069	0.020	0.011	0.002	0.003
Haarlem	162 517	0.008	0.007	<b>0.890</b>	0.021	0.006	0.053	0.010	0.001	0.003
Arnhem	162 413	0.009	0.030	0.021	0.051	<b>0.839</b>	0.018	0.023	0.001	0.008
Enschede	159 747	0.016	<b>0.905</b>	0.014	0.014	0.030	0.011	0.007	0.001	0.002
Haarlemmermeer	157 762	0.007	0.007	<b>0.842</b>	0.021	0.005	0.105	0.009	0.001	0.002
Amersfoort	157 446	0.015	0.029	0.064	<b>0.829</b>	0.016	0.030	0.014	0.002	0.003
Zaanstad	156 862	0.007	0.006	<b>0.932</b>	0.017	0.004	0.026	0.006	0.001	0.002
's-Hertogenbosch	155 463	0.004	0.006	0.017	0.034	0.024	0.022	<b>0.877</b>	0.003	0.013
Zwolle	129 857	0.053	<b>0.840</b>	0.030	0.033	0.017	0.017	0.007	0.001	0.002
Zoetermeer	125 223	0.006	0.006	0.031	0.020	0.005	<b>0.915</b>	0.013	0.002	0.002
Leeuwarden	124 493	<b>0.914</b>	0.022	0.027	0.013	0.005	0.012	0.005	0.001	0.001
Leiden	124 051	0.007	0.007	0.063	0.023	0.006	<b>0.876</b>	0.013	0.003	0.003
Maastricht	120 212	0.003	0.003	0.013	0.010	0.008	0.012	0.032	0.001	<b>0.917</b>
Dordrecht	119 112	0.005	0.006	0.018	0.025	0.006	<b>0.874</b>	0.057	0.006	0.004
Ede	118 541	0.010	0.030	0.024	<b>0.824</b>	0.060	0.030	0.016	0.003	0.004
Alphen a. d. Rijn	112 616	0.007	0.008	0.056	0.038	0.006	<b>0.868</b>	0.013	0.003	0.002
Westland	111 385	0.005	0.005	0.020	0.013	0.004	<b>0.937</b>	0.013	0.003	0.002
Alkmaar	109 886	0.010	0.007	<b>0.925</b>	0.016	0.004	0.028	0.007	0.001	0.002
Emmen	107 031	<b>0.908</b>	0.044	0.014	0.011	0.006	0.011	0.004	0.000	0.001
Delft	103 578	0.006	0.007	0.039	0.021	0.006	<b>0.897</b>	0.017	0.003	0.003
Venlo	101 968	0.002	0.004	0.008	0.009	0.026	0.009	0.053	0.001	<b>0.889</b>
Deventer	101 223	0.018	<b>0.845</b>	0.020	0.025	0.064	0.014	0.010	0.001	0.003
Helmond	92 629	0.002	0.004	0.009	0.011	0.015	0.013	<b>0.910</b>	0.001	0.034
Oss	92 542	0.003	0.006	0.010	0.027	0.066	0.013	<b>0.863</b>	0.001	0.010
Sittard-Geleen	91 728	0.002	0.003	0.008	0.008	0.008	0.010	0.036	0.001	<b>0.924</b>
Amstelveen	90 824	0.006	0.007	<b>0.902</b>	0.029	0.005	0.040	0.009	0.001	0.002